

---

# DA-TRANSUNET: INTEGRATING SPATIAL AND CHANNEL DUAL ATTENTION WITH TRANSFORMER U-NET FOR MEDICAL IMAGE SEGMENTATION \*

---

**Guanqun Sun**

School of Information Engineering  
 Hangzhou Medical College  
 Hangzhou, Zhejiang, 311399, China  
 School of Information Science  
 Japan Advanced Institute of Science and Technology  
 Nomi, Ishikawa, 923-1292, Japan  
 sun.guanqun@hmc.edu.cn

**Yizhi Pan**

School of Information Engineering  
 Hangzhou Medical College  
 Hangzhou, Zhejiang, 311399, China  
 panyizhi@hmc.edu.cn

**Weikun Kong**

Department of Electronic Engineering  
 Tsinghua University  
 Beijing, 100084, China  
 kong\_diison@mail.tsinghua.edu.cn

**Zichang Xu**

Immunology Frontier Research Institute  
 Osaka University  
 Suita 565-0871, Japan  
 xuzichang@biken.osaka-u.ac.jp

**Jianhua Ma**

Computer and Information Sciences  
 Hosei University  
 Tokyo184-8584, Japan  
 jianhua@hosei.ac.jp

**Teeradaj Racharak, Le-Minh Nguyen**

School of Information Science  
 Japan Advanced Institute of Science and Technology  
 Nomi, Ishikawa, 923-1292, Japan  
 {racharak, nguyenml}@jaist.ac.jp

**Junyi Xin**

School of Information Engineering  
 Hangzhou Medical College  
 Hangzhou, Zhejiang, 311399, China  
 ailab@hmc.edu.cn

## ABSTRACT

Great progress has been made in automatic medical image segmentation due to powerful deep representation learning. The influence of transformer has led to research into its variants, and large-scale replacement of traditional CNN modules. However, such trend often overlooks the intrinsic feature extraction capabilities of the transformer and potential refinements to both the model and the transformer module through minor adjustments. This study proposes a novel deep medical image segmentation framework, called DA-TransUNet, aiming to introduce the Transformer and dual attention block into the encoder and decoder of the traditional U-shaped architecture. Unlike prior transformer-based solutions, our DA-TransUNet utilizes attention mechanism of transformer and multifaceted feature extraction of DA-Block, which can efficiently combine global, local, and multi-scale features to enhance medical image segmentation. Meanwhile, experimental results show that a dual attention block is added before the Transformer layer to facilitate feature extraction in the U-net structure. Furthermore, incorporating dual attention blocks in skip connections can enhance feature transfer to the decoder, thereby improving image segmentation performance. Experimental results

---

\*Corresponding Author: Guanqun Sun, Le-Minh Nguyen, Junyi Xin

across various benchmark of medical image segmentation reveal that DA-TransUNet significantly outperforms the state-of-the-art methods. The codes and parameters of our model will be publicly available at <https://github.com/SUN-1024/DA-TransUnet>.

**Keywords** U-net · Medical Image Segmentation · Dual Attention · Transformer

## 1 Introduction

Precise delineation of lesions plays a crucial role in quantifying diseases, aiding the assessment of disease prognosis, and evaluating treatment efficacy. Manual segmentation is accurate and generally affordable for pathological diagnosis, but is crucial in a standardized clinical setting. Conversely, automated segmentation ensures a reliable and consistent process, boosting efficiency, cutting down on labor and costs, and preserving accuracy. Consequently, there is a substantial demand for exceptionally accurate automated medical image segmentation technology within the realm of clinical diagnostics.

In the last decade, Convolutional Neural Networks (CNNs) such as Fully Convolutional Network (FCN[1]), U-net[2] and its various improved models have achieved significant success. ResUNet[3] emerged during this period, influenced by the residual concept. Similarly UNet++[4] emphasizes enhancements in skip connections, and DAResUNet[5] incorporates a dual attention block with a residual block(Res-Block) in U-net. Both architectures have benefited from the influence of the encoder-decoder idea, while skip connections provide initial features for the decoder, bridging the semantic gap between encoders and decoders. However, limitations in the sensing field and biases in convolutional operations can compromise segmentation accuracy. Additionally, the inability to establish long-range dependencies and global context further constrains performance improvements. Importantly, the transformer [6], originally developed for sequence-to-sequence modeling in Natural Language Processing (NLP), has also found utility in the field of Computer Vision (CV). For example: visual transformers (ViTs) [7] have obtained good results by dividing an image into multiple small image modules, and then feeding a sequence of prior embeddings of these small image modules into the network as input to the transformer. The segmentation accuracy is further driven by the power of the transformer. Inspired by ViT, TransUNet[8] further combines the functionality of ViT with the advantages of U-net in the field of medical image segmentation. Specifically, it employs a transformer's encoder to process the image, and employs a conventional CNN and hopping connections for accurate up-sampling feature recovery. Swin-Unet[9] combines Swin-transform block with U-net structure and achieves good results. In the above mentioned work based on medical image segmentation, there are improvements based on the features of U-net and also based on transformers. To some extent, the above work is encouraging, but there are some limitations:

- 1) In the traditional U-shaped medical image segmentation model, the extended convolution process results in a deficiency of global information, marking global feature acquisition challenging.
- 2) With the introduction of the attention mechanism, numerous attention modules have been added to U-net. However, the challenge lies in optimally positioning and utilizing these modules to aid in feature extraction.
- 3) Transformer is powerful in extracting features while being able to retain global information. However, further stimulate the potential of Transformer and how to effectively combine the features of both CNN and Transformer is a question worth thinking about.
- 4) Skip connections are a very important part of the U-net model, bridging the semantic gap from the encoder to the decoder. The unresolved issue is optimizing these connections to enable the decoder to retrieve and return more precise feature maps, thereby enhancing the model's robustness.

With the problems and limitations mentioned above, we propose our model, DA-TransUNet. We believe that the extensive use of transformers isn't as impactful as utilizing a singular, optimized one. Thus, we focus on enhancing the integration of U-net and the transformer. To enhance feature accuracy within the transformer layer, we introduce a Dual Attention Block. This block integrates the Position Attention Block (PAM) and Channel Attention Block (CAM) from the Dual Attention Network for Scene Segmentation. Positioned in the embedding layer, the Dual Attention Block offers robust feature extraction capabilities. Considering the structure of the encoder-decoder and skip connection, we use Dual Attention Block for feature optimization of encoder-passed features in the three-layer skip connection, which helps the decoder-encoder structure to further reduce the semantic divide in order to generate a unified feature representation. This fusion approach can fully exploit different aspects, global and local features, and make them complementary to each other, thereby enhancing the model's medical image segmentation performance. Consistent with the traditional U-shaped structure, the encoder is used to obtain contextual features and skip connections and decoders are employed for the fusion of unified features. Unlike most CNN-based encoders, we include a Transformer module in the encoding to further extract contextual features at a distance to greatly improve the encoding capability, and to

improve the capability of the decoder, we further refine the features conveyed by the skip connections. Owing to these enhancements, both the decoding and medical image segmentation capabilities are significantly bolstered. We evaluated the effectiveness of DA-TransUNet using the CVC-ClinicDB dataset, the Kvasir SEG dataset, the Kvasir-Instrument dataset, the Synapse dataset and Chest X-ray mask and label dataset.

We mainly evaluate the effectiveness of proposed DA-TransUNet on several medical image datasets of Synapse[10], CVC-ClinicDB[11], ISIC2018[12][13], kvasir-seg[14], Kvasir-Instrument dataset[15] and Chest X-ray mask and label dataset[16] [17]. DA-TransUNet demonstrates notable efficacy, as evidenced by quantifiable metrics. Our main contributions are summarized below:

- 1) We propose DA-TransUNet, a novel architecture that integrates dual attention mechanisms for positional and channel information into a Transformer encoder-decoder framework. This approach improves the flexibility and functionality of the encoder-decoder structure, leading to enhanced performance in medical image segmentation tasks.
- 2) A well-designed dual-attention encoding mechanism is proposed to be positioned ahead of the Transformer layer, which can amplify its feature extraction capabilities and enrich the functionality of the encoder in the U-net structure.
- 3) We enhance the effectiveness of skip connections by incorporating Dual Attention Block into each layer, a modification substantiated by ablation studies, which results in more accurate feature delivery to the decoder and improved image segmentation performance.
- 4) Our proposed DA-TransUNet method achieves state-of-the-art performance on multiple medical imaging datasets, which proves the effectiveness of our method and its contribution to advancing medical image segmentation.

The rest of this article is organized as follows. Section II reviews the related works of automatic medical image segmentation, and the description of our proposed DA-TransUNet is given in Section III. Next, the comprehensive experiments and visualization analyses are conducted in Section IV. Finally, Section V makes a conclusion of the whole work.

## 2 Related Work

### 2.1 U-net Model

Recently, attention mechanisms have gained popularity in U-net architectures[2]. For example, Attention U-net incorporates attention mechanisms to enhance pancreas localization and segmentation performance[18]; DAREsUNet integrates both double attention and residual mechanisms into U-net [5]; Attention Res-UNet explores the substitution of hard-attention with soft-attention [19]; Sa-unet incorporates a spatial attention mechanism in U-net[20]. Following this, TransUNet innovatively combines Transformer and U-net elements [8]. Building on TransUNet, TransU-Net++ incorporates attention mechanisms into both skip connections and feature extraction[21]. Swin-Unet[9] improves by replacing every convolution block in U-net with Swin-Transformer[22]. DS-TransUNet proposes to incorporate the tif module to the skip connection to improve the model[23]. AA-transunet leverages Block Attention Model (CBAM) and Deep Separable Convolution (DSC) to further optimize TransUNet [24]. TransFuse uses dual attention Bifusion blocks and AG to fuse features of two different parts of CNN and Transformer[25]. Numerous attention mechanisms have been added to U-net and TransUNet models, yet further exploration is warranted. Diverging from prior approaches, our experiment introduces a dual attention mechanism and Transformer module into the traditional U-shaped encoder-decoder and skip connections, yielding promising results.

### 2.2 Application of skip connections in medical image segmentation modeling

Skip connections in U-net aim to bridge the semantic gap between the encoder and decoder, effectively recovering fine-grained object details [26][27][28]. There are three primary modifications to skip connections: firstly, increasing their complexity [29]. U-Net++ redesigned the skip connection to include a Dense-like structure in the skip connection[4], and U-Net3++[30] changed the skip connection to a full-scale skip connection. Secondly, RA-UNet introduces a 3D hybrid residual attention-aware method for precise feature extraction in skipped connections [31]. The third is a combination of encoder and decoder feature maps: An alternative extension to the classical skip connection was introduced in BCDU-Net with a bidirectional convolutional long-term-short-term memory (LSTM) module was added to the skip connection[32]. Aligning with the second approach, we integrate Dual Attention Blocks into each skip connection layer, enhancing decoder feature extraction and thereby improving image segmentation accuracy.

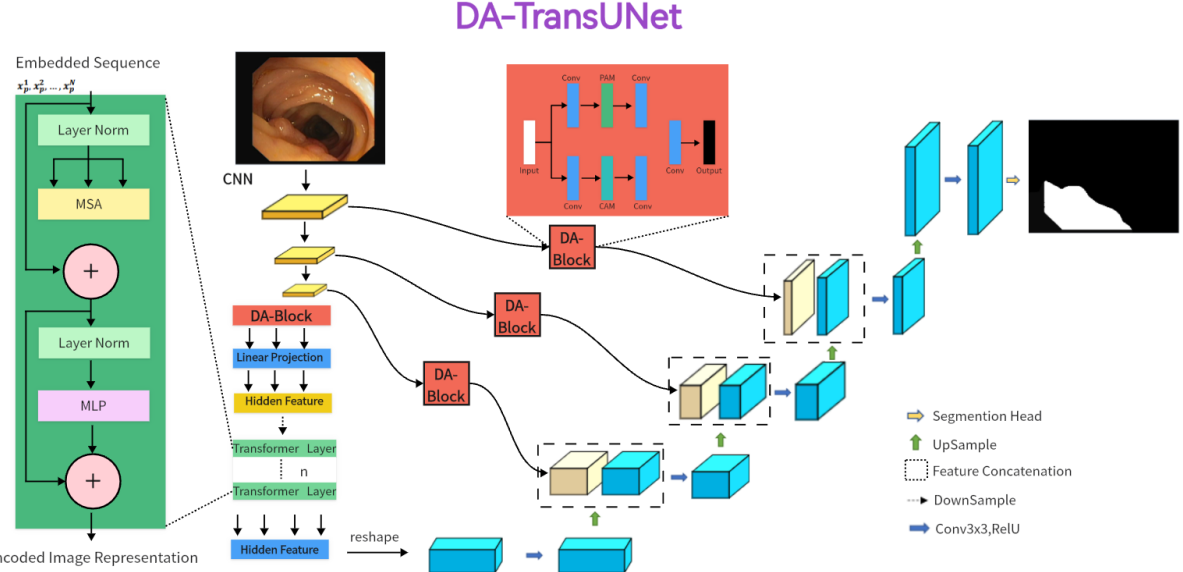


Figure 1: Illustration of the proposed dual attention transformer U-Net(DA-TransUNet). For the input medical images, we feed them into an encoder with transformer and Dual Attention Block (DA-Block). Then, the features of each of the three different scales are purified by DA-Block. Finally, the purified skip connections are fused with the decoder, which subsequently undergoes CNN-based up-sampling to restore the channel to the same resolution as the input image. In this way, the final image prediction result is obtained.

### 2.3 The use of attentional mechanisms in medical images

Attention mechanisms are essential for directing model focus towards relevant features, thereby enhancing performance. In recent years, dual attention mechanisms have seen diverse applications across multiple fields. In scene segmentation, the Dual Attention Network (DANet) employs spatial and channel attention mechanisms to improve performance [33]. A modularized DANs framework is presented that adeptly merges visual and textual attention mechanisms [34]. This cohesive approach enables selective focus on pivotal features in both types of data, thereby improving task-specific performance. Additionally, the introduction of the Dual Attention Module (DuATM) has been groundbreaking in the field of audio-visual event localization. This model excels at learning context-aware feature sequences and performing attention sequence comparisons in tandem, effectively incorporating auditory-oriented visual attention mechanisms [35]. Moreover, dual attention mechanisms have been applied to medical segmentation, yielding promising results[36]. The Multilevel Dual Attention U-net for Polyp Segment combines dual attention and U-net in medical image segmentation[37]. While significant progress has been made in medical image segmentation, there is still ample room for further research to explore the potential of dual attention blocks in the field of medical image segmentation.

## 3 Method

In the subsequent section, we propose the DA-TransUNet architecture, as visualized in Figure.1. We begin with an overview of the overall architecture. We then elaborate on its principal components in the following order: the dual attention blocks, uniquely serving as specialized feature extraction modules, the encoder, the skip connections, and finally, the decoder.

### 3.1 Overview of DA-TransUNet

Expanding upon Figure.1, we outline the DA-TransUNet architecture. The model is organized into three core segments: the encoder, the decoder, and the skip connections. In particular, the encoder fuses a conventional convolutional neural network (CNN) with a Transformer layer and is further enriched by the dual attention blocks, which are exclusively introduced in this architecture. In contrast, the decoder primarily employs conventional convolutional mechanisms. The dual attention blocks are pivotal in enabling efficient skip connections. The objective of the DA-TransUNet architecture is to augment image segmentation performance. It achieves this by synergistically integrating traditional

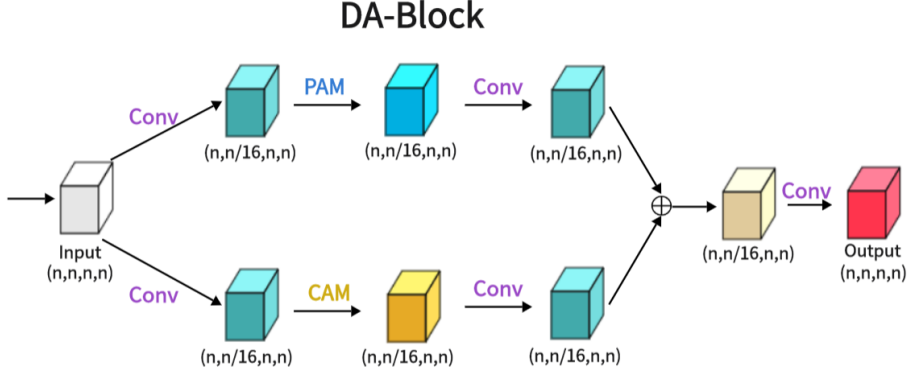


Figure 2: The proposed Dual Attention Block (DA-Block) is shown in the Figure. The same input feature map is input into two feature extraction layers, one is the position feature extraction block and the other is the channel feature extraction block, and finally, the two different features are fused to obtain the final DA-Block output.

convolutional mechanisms, Transformer layers, and specialized dual-attention blocks. Concurrently, the architecture employs skip-connections to facilitate superior feature extraction and accurate restoration of the input image.

To elucidate the rationale behind our proposed DA-TransUNet model's design, it's imperative to consider the limitations and strengths of both U-Net architectures and Transformers in the context of feature extraction. While Transformers excel in global feature extraction through their self-attention mechanisms, they are inherently limited to unidirectional focus on positional attributes, thus neglecting multi-faceted feature perspectives. On the other hand, traditional U-Net architectures are proficient in local feature extraction but lack the capability for comprehensive global contextualization. To address these constraints, we integrate Directional Attention Block (DA-Block) both preceding the Transformer layers and within the encoder-decoder skip connections. This serves dual purposes: firstly, it refines the feature map input to the Transformer, enabling more nuanced and precise global feature extraction; secondly, the DA-Block in the skip connections optimize the transmitted features from the encoder, facilitating the decoder in reconstructing a more accurate feature map. Thus, our proposed architecture amalgamates the strengths and mitigates the weaknesses of both foundational technologies, resulting in a robust system capable of multi-angle feature extraction.

Next, we detail the operational flow of the DA-TransUNet model. Initially, the input image undergoes three cycles of convolution and downsampling, resulting in a feature map of dimensions (1024,14,14). A convolutional dual-attention block is then deployed for feature extraction, diminishing the dimensions to (768,14,14). We chose these dimensions to maintain a balance between computational efficiency and feature expressiveness. The feature map is subsequently flattened from a three-dimensional to a two-dimensional array (196,768) and fed into the Transformer layers, which output features of the same dimensions. This flattening step allows the Transformer to process the features more effectively due to its native two-dimensional input requirement. These are then reverted back to a three-dimensional shape (768,14,14). This reshaped feature map is used as input for the decoder. The decoder employs three stages of upsampling, convolution, and skip-connections to produce a feature map of shape (64,112,112). The three-stage design was chosen to gradually refine the features while upsampling, providing a more accurate reconstruction. A final upsampling step restores the image to its original dimensions.

### 3.2 Dual Attention Block(DA Block)

As shown in the attached Figure 2, the Dual Attention Block (DA-Block) is a feature extraction module that integrates both location-based and channel-based feature extraction components, allowing for feature extraction from two different perspectives. Extracting features from various angles enhances the precision and granularity of the obtained features. While the Transformer possesses excellent feature extraction capabilities, focusing on different positions, it may overlook the requirement for precision in medical images. In contrast, the DA-Block excels not only in position-based feature extraction but also in channel-based feature extraction. Compared to single-feature extraction, multi-angle feature extraction can acquire more accurate and detailed features, thereby improving the model's segmentation capabilities. Therefore, we incorporate it into the encoder and skip connections to enhance the model's segmentation performance. The DA-Block consists of two primary components: one featuring a Position Attention Module (PAM), and the other incorporating a Channel Attention Module (CAM), both borrowed from the Dual Attention Network for scene segmentation[33].

**PAM (Position Attention Module):** As shown in Figure 3, this is the PAM, which can capture spatial dependencies between any two positions of feature maps, updating specific features through a weighted sum of all position features. The weights are determined by the feature similarity between two positions. Therefore, PAM is effective at extracting meaningful spatial features.

PAM initially takes a local feature, denoted as  $A \in R^{C \times H \times W}$  (C represents Channel, H represents height, and W represents Width). We then feed A into a convolutional layer, resulting in three new feature maps, namely B, C, and D, each of size  $R^{C \times H \times W}$ . Next, we reshape B and C to  $R^{C \times N}$ , where  $N = H \times W$  denotes the number of pixels. We perform a matrix multiplication between the transpose of C and B and subsequently use a softmax layer to compute the spatial attention map  $S \in R^{N \times N}$ :

$$S_{ji} = \frac{\exp(B_i \cdot C_j)}{\sum_{i=1}^N \exp(B_i \cdot C_j)} \quad (1)$$

Here,  $S_{ji}$  measures the impact of the i-th position on the j-th position. We then reshape matrix D to  $R^{C \times N}$ . A matrix multiplication is performed between D and the transpose of S, followed by reshaping the result to  $R^{C \times H \times W}$ . Finally, we multiply it by a parameter  $\alpha$  and perform an element-wise sum operation with the features A to obtain the final output  $E \in R^{C \times H \times W}$ :

$$E_j = \alpha \sum_{i=1}^N (s_{ji} D_i) + A_j \quad (2)$$

The weight  $\alpha$  is initialized as 0 and is learned progressively. PAM has a strong capability to extract spatial features. As E is generated as a weighted sum of all position features and original features, it possesses global contextual features and aggregates context based on the spatial attention map. This ensures effective extraction of position features while maintaining global contextual information.

**CAM (Channel Attention Module):** As shown in Figure 4, this is CAM, which excels in extracting channel features. Unlike PAM, we directly reshape the original feature  $A \in R^{C \times H \times W}$  to  $R^{C \times N}$ , and then perform a matrix multiplication between A and its transpose. Subsequently, we apply a softmax layer to obtain the channel attention map  $X \in R^{C \times C}$ :

$$x_{ji} = \frac{\exp(A_i \cdot A_j)}{\sum_{i=1}^C \exp(A_i \cdot A_j)} \quad (3)$$

Here,  $x_{ji}$  measures the impact of the i-th channel on the j-th channel. Next, we perform a matrix multiplication between the transpose of X and A, reshaping the result to  $R^{C \times H \times W}$ . We then multiply the result by a scale parameter  $\beta$  and perform an element-wise sum operation with A to obtain the final output  $E \in R^{C \times H \times W}$ :

$$E_j = \beta \sum_{i=1}^N (x_{ji} A_i) + A_j \quad (4)$$

Like  $\alpha$ ,  $\beta$  is learned through training. Similar to PAM, during the extraction of channel features in CAM, the final feature for each channel is generated as a weighted sum of all channels and original features, thus endowing CAM with powerful channel feature extraction capabilities.

**DA (Dual Attention Module):** As shown in the Figure 2, we present the architecture of the Dual Attention Block (DA-Block). This architecture merges the robust position feature extraction capabilities of the Positional Attention Module (PAM) with the channel feature extraction strengths of the Channel Attention Module (CAM). Furthermore, when coupled with the nuances of traditional convolutional methodologies, the DA-Block emerges with superior feature extraction capabilities. DA-Block consists of two layers, the first one is dominated by PAM and the second one is dominated by CAM. The first layer first takes the input features and performs one convolution to scale the number of channels by one-sixteenth to get  $\alpha^1$ , which can help the PAM block extract the features more easily, and then after one feature extraction of the PAM block and one ordinary convolution to get  $\hat{\alpha}^1$

$$\alpha^1 = \text{Conv}(\text{input}) \quad (5)$$

$$\hat{\alpha}^1 = \text{Conv}(\text{PAM}(\alpha^1)) \quad (6)$$

The other layer is the same, with the only difference being that the PAM block is replaced with a CAM with the following formula:

$$\alpha^2 = \text{Conv}(\text{input}) \quad (7)$$

$$\hat{\alpha}^2 = \text{Conv}(\text{CAM}(\alpha^2)) \quad (8)$$

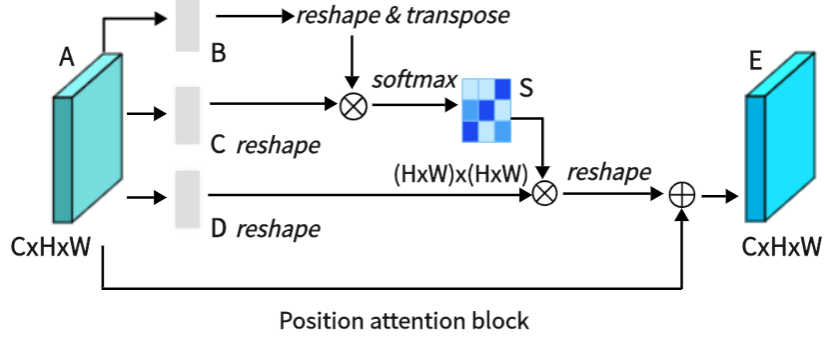


Figure 3: Architecture of Position Attention Mechanism(PAM).

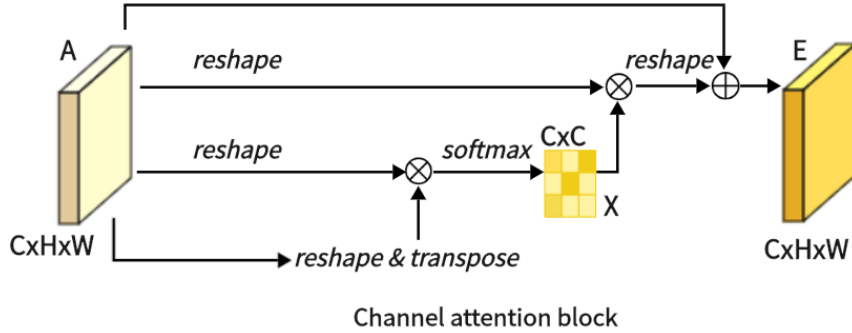


Figure 4: Architecture of Channel Attention Mechanism(CAM).

After extracting  $\hat{\alpha}^1$  and  $\hat{\alpha}^2$  from the two layers of attention, the output is obtained by aggregating and summing the two layers of attention and recovering the number of channels in one convolution.

$$output = Conv(\hat{\alpha}^1 + \hat{\alpha}^2) \quad (9)$$

This sophisticated DA Block architecture seamlessly integrates the strengths of the Position Attention Module and Channel Attention Module to improve feature extraction, making it a critical component in enhancing the model's overall performance.

### 3.3 Encoder with Transformer and Dual Attention

Illustrated in Figure 1, the encoder architecture consists of three key components: three convolutional blocks, dual-attention modules, an embedding layer, and layers dedicated to the Transformer. Particularly crucial is the inclusion of a DA-Block before the Transformer layer. This design choice was influenced by the need to purify the features obtained through three convolutional blocks, making them more suitable for global feature extraction by the Transformer. The Transformer architecture plays a cardinal role in the preservation of global context, while the DA block empowers the Transformer's feature acquisition, amplifying its adeptness in capturing potent global contextual information. This synergistic approach harmoniously amalgamates both global and localized features, effectively harmonizing their integration. The composition of the three convolutional blocks conforms to the architecture of the U-Net and its diverse iterations, seamlessly integrating convolutional operations with downsampling processes. Each convolutional layer halves the size of the input feature map and doubles its dimension, a configuration empirically found to maximize feature expressiveness while maintaining computational efficiency. Dual-attention modules extract features at both positional and channel levels, enhancing the depth of feature representation while preserving the intrinsic characteristics of the input map. The embedding layer serves as a critical intermediary, enabling the requisite dimensional adaptation, a prelude to the subsequent Transformer strata. The integration of Transformer layers was a strategic choice to furnish the model with adept global feature extraction, something traditional CNN layers could not achieve alone. Within the bounds of the encoder division, the input image traverses three consecutive convolutional blocks, systematically expanding the receptive field to encompass vital features. Subsequently, the DA-Block refines features through the

application of both position-based and channel-based attention mechanisms. Following this, the remodeled features undergo a dimensionality transformation courtesy of the embedding stratum before they are channeled into the Transformer framework for the extraction of all-encompassing global features. This orchestrated progression safeguards the comprehensive retention of information across the continuum of successive convolutional layers. Ultimately, the feature map generated by the Transformer is restructured and guided through intermediate strata en route to the decoder.

By amalgamating convolutional neural networks, transformer architectures, and dual-attention mechanisms, the encoder configuration culminates in a robust capability for feature extraction, resulting in a symbiotic powerhouse of capabilities.

### 3.4 Skip-connections with Dual Attention

Similar to other U-structured models, we have also incorporated skip connections between the encoder and decoder to bridge the semantic gap that exists between them. To further minimize this semantic gap, we introduced dual-attention blocks (DA-Blocks), as depicted in Figure 1, in each of the three skip connection layers. This decision was based on our observation that traditional skip connections often transmit redundant features, which Da-Blocks effectively filter. Integrating DA-Blocks into the skip connections allows them to refine the sparsely encoded features from both positional and channel perspectives, extracting more valuable information while reducing redundancy. By doing so, Da-Blocks assist the decoder in more accurate feature map reconstruction. Moreover, the inclusion of Da-Blocks not only enhances the model’s robustness but also effectively mitigates sensitivity to overfitting, contributing to the overall performance and generalization capability of the model.

### 3.5 Decoder

As shown in Figure 1, the right half of the diagram represents the decoder. The decoder’s primary function is to reconstruct the original feature maps from the features obtained through the encoder and those received via skip connections, using operations such as upsampling. This reconstruction is essential for preserving semantic information while restoring spatial details in the image. Therefore, we employ skip connections and the decoder to restore the original feature maps.

The decoder architecture consists of feature fusion, segmentation heads, and three upsampling convolutional blocks. Feature fusion involves the integration of feature maps passed through skip connections with existing feature maps. Segmentation heads are responsible for restoring the feature maps to their original dimensions. The three upsampling convolutional blocks increase the size of the input feature maps by a factor of 2 in each step. Within the scope of the decoder, the workflow involves passing the input image through a convolutional block followed by upsampling, which increases the size of the feature maps by a factor of two and reduces their dimensions by half. Then, the features transmitted through skip connections are fused, and the upsampling and convolution continue. After three cycles of this process, the resulting feature maps undergo one final upsampling and pass through a segmentation head to restore them to their original size.

With this architecture, the decoder exhibits robust decoding capabilities and can effectively recover the original feature maps based on the features from the encoder and skip connections.

## 4 Experiments

To evaluate the proposed method, we performed experiments on Synapse[10], CVC-ClinicDB dataset[11], Chest X-ray mask and label dataset[16] [17] Analysis, Kvasir SEG dataset[14], Kvasir-Instrument dataset[15], 2018ISIC-Task[12][13]. The experimental results demonstrate that DA-TransUNet outperforms existing methods across all six datasets. In the following subsections, we first introduce the dataset and implementation details. Finally, we report experimental results on Synapse, CVC-ClinicDB, Chest X-ray Mask and Tag, Kvasir SEG, Kvasir-Instrument and 2018ISIC-Task.

### 4.1 Datasets

#### 4.1.1 Synapse

The Synapse dataset consists of 30 scans of eight abdominal organs. This eight organs include the left kidney, right kidney, aorta, spleen, gallbladder, liver, stomach and pancreas. There are a total of 3779 axially enhanced abdominal clinical CT images.

#### 4.1.2 CVC—ClinicDB

CVC-ClinicDB is a database of frames extracted from colonoscopy videos, which is part of the Endoscopic Vision Challenge. This is a dataset of endoscopic colonoscopy frames for the detection of polyps. CVC-ClinicDB contains 612 still images from 29 different sequences. Each image has its associated manually annotated ground truth covering the polyp.

#### 4.1.3 Chest Xray

Chest Xray Masks and Labels X-ray images and corresponding masks are provided. The X-rays were obtained from the Montgomery County Department of Health and Human Services Tuberculosis Control Program, Montgomery County, Maryland, USA. The set of images contains 80 anterior and posterior X-rays, of which 58 X-rays are normal and 1702 X-rays are abnormal with evidence of tuberculosis. All images have been de-identified and presented in DICOM format. The set contains a variety of abnormalities, including exudates and corneal morphology. It contains 138 posterior anterior radiographs, of which 80 radiographs were normal and 58 radiographs showed abnormal manifestations of tuberculosis.

#### 4.1.4 Kvasir SEG

Kvasir SEG is an open-access dataset of gastrointestinal polyp images and corresponding segmentation masks, manually annotated and verified by an experienced gastroenterologist. It contains 1000 polyp images and their corresponding ground truth, the resolution of the images contained in Kvasir-SEG varies from 332x487 to 1920x1072 pixels, the file format is jpg.

#### 4.1.5 Kvasir-Instrument

Kvasir-Instrument a gastrointestinal instrument Dataset. It contains 590 endoscopic tool images and their ground truth mask, the resolution of the image in the dataset varies from 720x576 to 1280x1024, which consists of 590 annotated frames comprising of GI procedure tools such as snares, balloons, biopsy forceps, etc. the file format is jpg.

#### 4.1.6 2018ISIC-Task

The dataset used in the 2018 ISIC Challenge addresses the challenges of skin diseases. It comprises a total of 2512 images, with a file format of JPG. The images of lesions were obtained using various dermatoscopic techniques from different anatomical sites (excluding mucous membranes and nails). These images are sourced from historical samples of patients undergoing skin cancer screening at multiple institutions. Each lesion image contains only a primary lesion.

### 4.2 Implementation Settings

#### 4.2.1 Baselines

In our endeavor to innovate in the field of medical image segmentation, we benchmark our proposed model against an array of highly-regarded baselines, including the U-net, UNet++, DA-Unet, Attention U-net, and TransUNet. The U-net has been a foundational model in biomedical image segmentation[2]. The UNet++ brings added sophistication with its implementation of intermediate layers[4]. The DA-Unet goes a step further by integrating dual attention blocks, amplifying the richness of features extracted[37]. The Attention U-net employs an attention mechanism for improved feature map weighting[18], and finally, the TransUNet deploys a transformer architecture, setting a new bar in segmentation precision[8]. Through this comprehensive comparison with these eminent baselines, we aim to highlight the unique strengths and expansive potential applications of our proposed model. Additionally, we benchmarked our model against advanced state-of-the-art algorithms. UCTansNet allocates skip connections through the attention module in the traditional U-net model[38]. TransNorm integrates the Transformer module into the encoder and skip connections of standard U-Net [39]. A novel Transformer module was designed and a model named MIM was built with it [40]. By extensively comparing our model with current state-of-the-art solutions, we intend to showcase its superior segmentation performance.

#### 4.2.2 Implementation Details

We implemented DA-TransUNet using the PyTorch framework and trained it on a single NVIDIA RTX 3090 GPU [41]. The model was trained with an image resolution of 256x256 and a patch size of 16. We employed the Adam optimizer, configured with a learning rate of 1e-3, momentum of 0.9, and weight decay of 1e-4. All models were trained for 500

Table 1: Experimental results on the Synapse dataset

Model	Year	DSC↑	HD↓	Aorta	Gallbladder	Kidney(L)	Kidney(R)	Liver	Pancreas	Spleen	Stomach
U-net	2015	76.85%	39.70	89.07	<b>69.72</b>	77.77	68.6	93.43	53.98	86.67	75.58
U-Net++	2018	76.91%	36.93	88.19	68.89	81.76	75.27	93.01	58.20	83.44	70.52
Residual U-Net	2018	76.95%	38.44	87.06	66.05	<b>83.43</b>	76.83	93.99	51.86	85.25	70.13
Att-Unet	2018	77.77%	36.02	<b>89.55</b>	68.88	77.98	71.11	93.57	58.04	87.30	75.75
MultiResUNet	2020	77.42%	36.84	87.73	65.67	82.08	70.43	93.49	60.09	85.23	75.66
TransUNet	2021	77.48%	31.69	87.23	63.13	81.87	77.02	94.08	55.86	85.08	75.62
UCTransNet	2022	78.23%	26.75	84.25	64.65	82.35	77.65	94.36	58.18	84.74	79.66
TransNorm	2022	78.40%	30.25	86.23	65.1	82.18	78.63	94.22	55.34	89.50	76.01
MIM	2022	78.59%	26.59	87.92	64.99	81.47	77.29	93.06	59.46	87.75	76.81
swin-unet	2022	79.13%	<b>21.55</b>	85.47	66.53	83.28	79.61	94.29	56.58	<b>90.66</b>	76.60
<b>DA-TransUNet(Ours)</b>	2023	<b>79.80%</b>	23.48	86.54	65.27	81.70	<b>80.45</b>	<b>94.57</b>	<b>61.62</b>	88.53	<b>79.73</b>

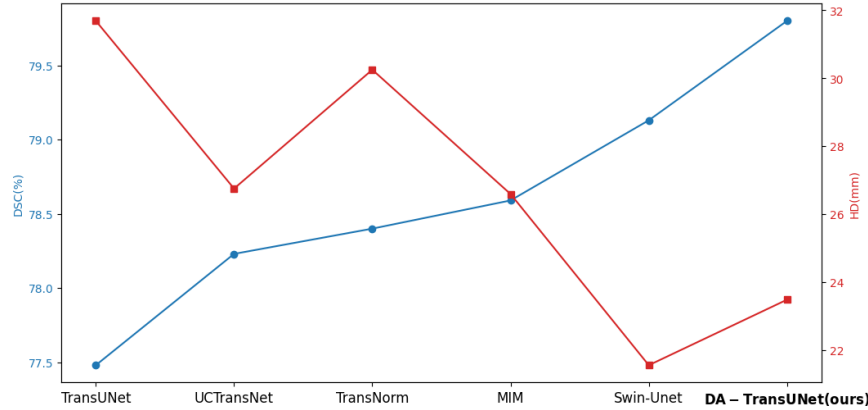


Figure 5: Line chart of DSC and HD values of several advanced models in the Synapse dataset

Table 2: Experimental results of datasets (CVC-ClinicDB, Chest Xray Masks and Labels, ISIC2018-Task, kvasir-instrument, kvasir-seg)

	CVC-ClinicDB		Chest Xray Masks and Labels		ISIC2018-Task		kvasir-instrument		kvasir-seg	
	Iou↑	Dice↑	Iou↑	Dice↑	Iou↑	Dice↑	Iou↑	Dice↑	Iou↑	Dice↑
U-net	0.7821	0.8693	0.9303	0.9511	0.8114	0.8722	0.8957	0.9358	0.8012	0.8822
Attn-Unet	0.7935	0.8741	0.9274	0.9503	0.8151	0.876	0.8949	0.9359	0.7801	0.8661
Unet++	0.7847	0.8714	0.9289	0.9505	0.8133	0.873	<b>0.8995</b>	<b>0.9389</b>	0.7767	0.8657
ResUNet	0.5902	0.7422	0.9262	0.9505	0.7651	0.8332	0.8572	0.9141	0.6604	0.7785
TransUNet	0.8163	0.8901	0.9301	0.9535	0.8263	0.8878	0.8926	0.9363	0.8003	0.8791
<b>DA-TransUNet(Ours)</b>	<b>0.8251</b>	<b>0.8947</b>	<b>0.9317</b>	<b>0.9538</b>	<b>0.8278</b>	<b>0.8888</b>	0.8973	0.9381	<b>0.8102</b>	<b>0.8847</b>

epochs unless stated otherwise. In order to ensure the convergence of the indicators, but due to different data set sizes, we used 50 epochs for training on the two data sets, Chest Xray Masks and Labels and ISIC 2018-Task.

During the training phase on five datasets, including CVC-ClinicDB, the proposed DA-TransUNet model is trained in an end-to-end manner. Its objective function consists of a weighted binary cross-entropy loss function (BCE) and a Dice coefficient loss function. To facilitate training, the final loss function, termed "Loss," is formulated as follows:

$$\text{Loss} = \frac{1}{2} \times \text{BCE} + \frac{1}{2} \times \text{DiceLoss} \quad (10)$$

To ensure a fair evaluation of the Synapse dataset, we utilized the pre-trained model "R50-ViT" with input resolution and patch size set to 224x224 and 16, respectively. We trained the model using the SGD optimizer, setting the learning rate to 0.01, momentum of 0.9, and weight decay of 1e-4. The default batch size was set to 24. The loss function employed for the Synapse dataset is defined as follows:

$$\text{Loss} = \frac{1}{2} \times \text{Cross-Entropy Loss} + \frac{1}{2} \times \text{DiceLoss} \quad (11)$$

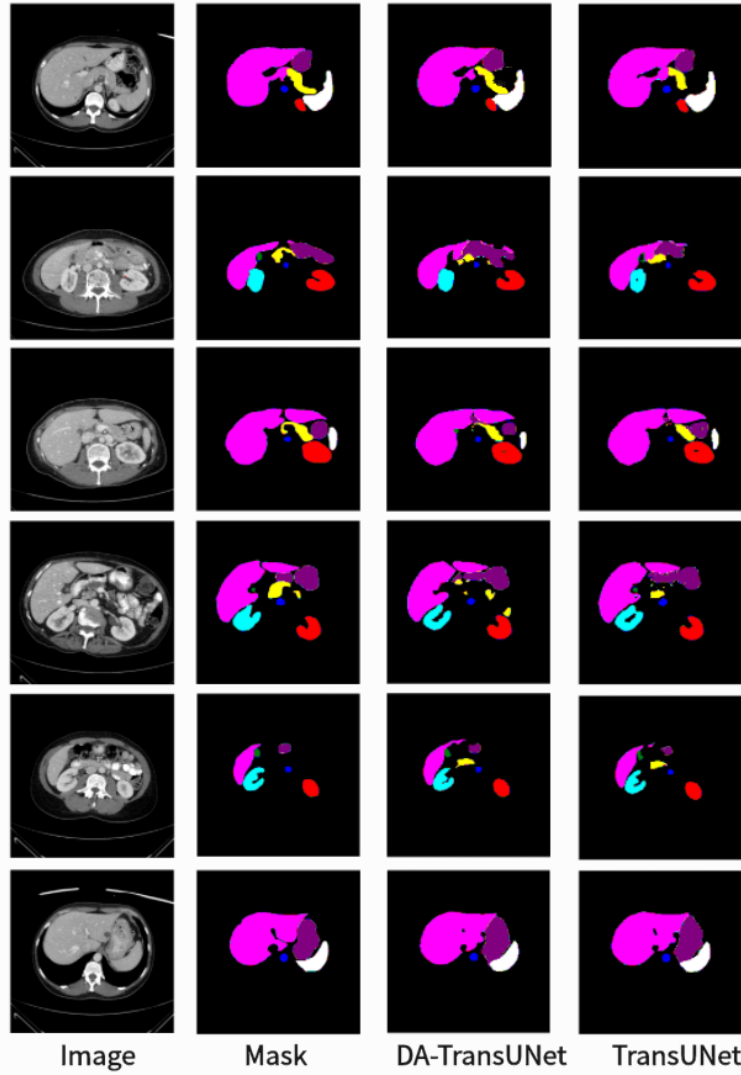


Figure 6: Segmentation results of TransUNet and DA-TransUNet on the Synapse dataset.

This loss function balances the contributions of cross-entropy and Dice losses, ensuring impartial evaluation during testing on the Synapse dataset.

When using the datasets, we use a 3 to 1 ratio, where 75% is the training set and 25% is the test set, to ensure adequacy of training.

#### 4.2.3 Model Evaluation

In evaluating the performance of DA-TransUNet, we utilize a comprehensive set of metrics including Intersection over Union (IoU), Dice Coefficient(DSC), and Hausdorff Distance (HD). These metrics are industry standards in computer vision and medical image segmentation, providing a multifaceted assessment of the model's accuracy, precision, and robustness.

IOU (Intersection over Union) is one of the commonly used metrics to evaluate the performance of computer vision tasks such as object detection, image segmentation and instance segmentation. It measures the degree of overlap between the predicted region of the model and the actual target region, which helps us to understand the accuracy and precision of the model. In target detection tasks, IOU is usually used to determine the degree of overlap between the predicted bounding box (Bounding Box) and the real bounding box. In image segmentation and instance segmentation

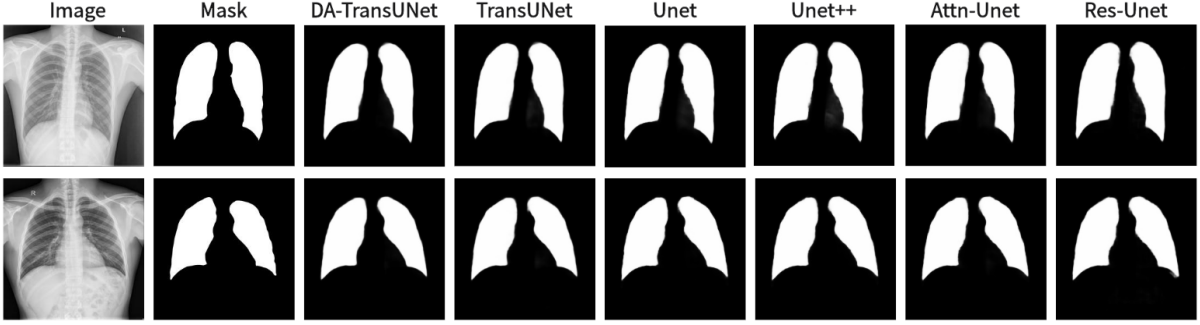


Figure 7: Comparison of qualitative results between DA-TransUNet and existing models on the task of segmenting Chest X-ray Masks and Labels X-ray datasets.

tasks, IOU is used to evaluate the degree of overlap between the predicted region and the ground truth segmentation region.

$$IOU = \frac{TP}{FP + TP + FN} \quad (12)$$

The Dice coefficient (also known as the Sørensen-Dice coefficient, F1-score, DSC) is a measure of model performance in image segmentation tasks, and is particularly useful for dealing with class imbalance problems. It measures the degree of overlap between the predicted results and the ground truth segmentation results, and is particularly effective when dealing with segmentation of objects with unclear boundaries. The Dice coefficient is commonly used as a measure of the model's accuracy on the target region in image segmentation tasks, and is particularly suitable for dealing with relatively small or uneven target regions.

$$\text{Dice}(P, T) = \frac{|P_1 \cap T_1|}{|P_1| + |T_1|} \Leftrightarrow \text{Dice} = \frac{2|T \cap P|}{|F| + |P|} \quad (13)$$

Hausdorff Distance (HD) is a distance measure for measuring the similarity between two sets and is commonly used to evaluate the performance of models in image segmentation tasks. It is particularly useful in the field of medical image segmentation to quantify the difference between predicted and true segmentations. The computation of Hausdorff distance captures the maximum difference between the true segmentation result and the predicted segmentation result, and is particularly suitable for evaluating the performance of segmentation models in boundary regions.

$$H(A, B) = \max \left\{ \max_{a \in A} \min_{b \in B} \|a - b\|, \max_{b \in B} \min_{a \in A} \|b - a\| \right\} \quad (14)$$

We evaluate using both Dice and HD in the Synapse dataset and both Dice and IOU in other datasets.

### 4.3 Comparison to the State-of-the-Art Methods

We have chosen U-net[2], Res-Unet[3], TransUNet[8], U-Net++[4], Att-Unet[18], TransNorm[39], UCTransNet[38], MultiResUNet[42], swin-unet[9] and MIM[40] to compare with our DA-TransUNet, and the experimental data are tabulated below.

In order to demonstrate the superiority of the DA-TransUNet model proposed in this paper, we conducted the main experiments using the Synapse dataset and compared it with its 11 state-of-the-art models (SOTA) (see table1).

As shown in the Figure6, we can see that the average DSC and average HD evaluation criteria are 79.80% and 23.48 mm, respectively, which are improved by 2.32% and 8.21 mm, respectively, compared with TransUNet, which indicates that our DA-TransUNet has better segmentation ability than TransUNet in terms of overall segmentation results and organ edge prediction. As shown in the Figure5, on the other hand, we can see that DSC has the highest value of our model. Although HD is higher than Swin-Unet, it is still an improvement compared to several newer models and TransUNet. The segmentation time for an image is 35.98 ms for our DA-TransUNet and 33.58 ms for TransUNet, which indicates that there is not much difference in the segmentation speed between the two models, but our DA-TransUNet has better

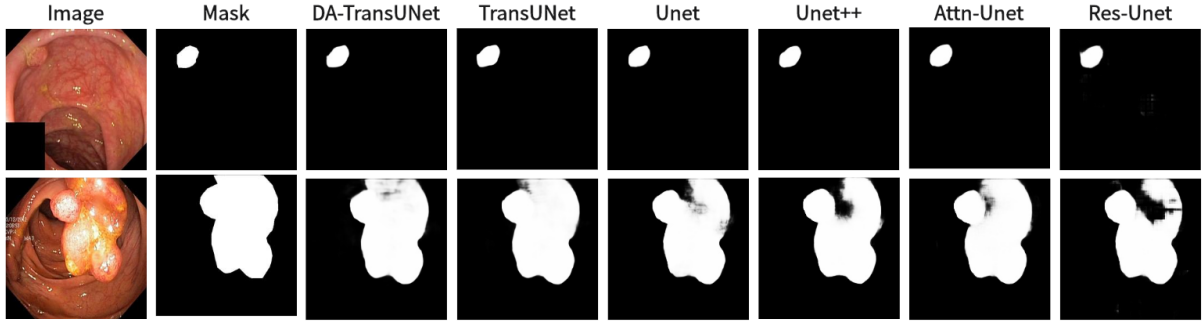


Figure 8: Comparison of qualitative results between DA-TransUNet and existing models on the task of segmenting Kvasir-Seg datasets.

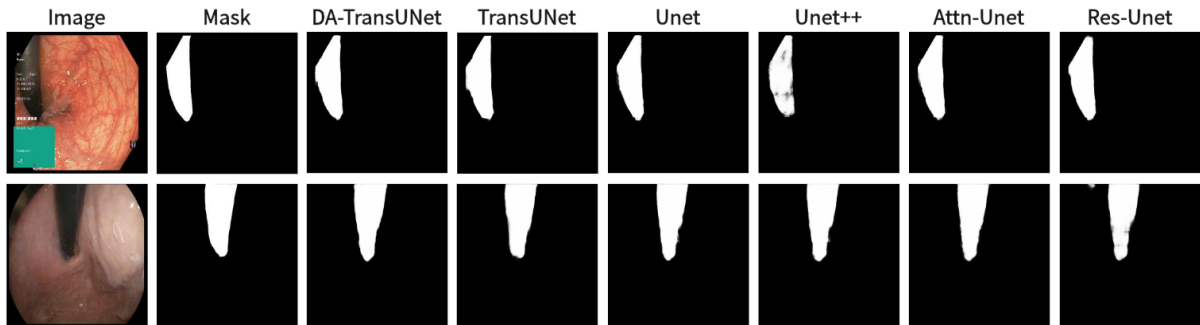


Figure 9: Comparison of qualitative results between DA-TransUNet and existing models on the task of segmenting Kavsir-Instrument datasets.

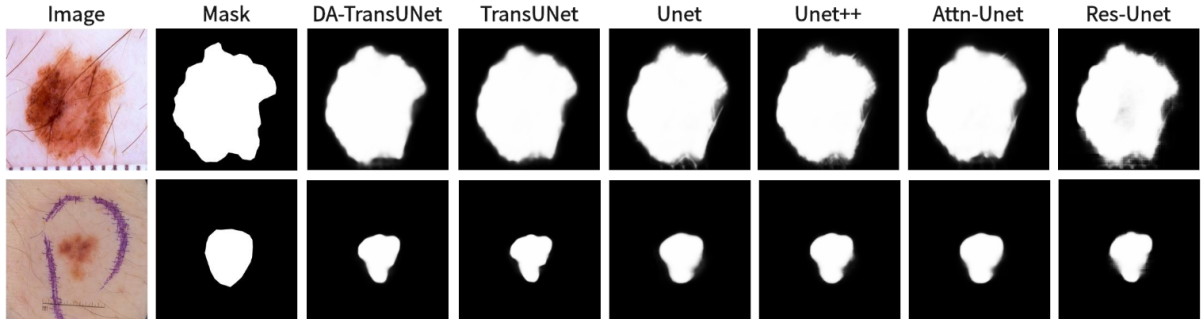


Figure 10: Comparison of qualitative results between DA-TransUNet and existing models on the task of segmenting 2018ISIC-Task datasets.

segmentation results. In the segmentation results of 8 organs, DA-TransUNet outperforms TransUNet by 2.14%, 3.43%, 0.48%, 3.45%, and 4.11% for the five datasets of Gallbladder, right kidney, liver, spleen, and stomach, respectively. The segmentation rate for the pancreas is notably higher at 5.73%. In a comparative evaluation across six distinct organs, DA-TransUNet demonstrates superior segmentation capabilities relative to TransUNet. Nevertheless, it exhibits a marginal decrement in the segmentation accuracy for the aorta and left kidney by 0.69% and 0.17%, respectively. The model achieves the best segmentation rates for the right kidney, liver, pancreas, and stomach, indicating superior feature learning capabilities on these organs.

To further confirm the better segmentation of our model compared to TransUNet, we visualized the segmentation plots of TransUNet and DA-TransUNet (see Figure6). From the yellow and purple parts in the first column, we can see that

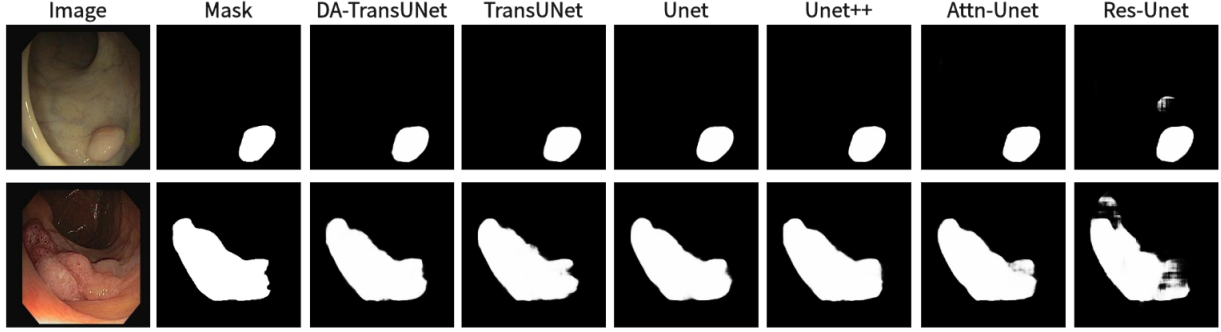


Figure 11: Comparison of qualitative results between DA-TransUNet and existing models on the task of segmenting CVC-ClinicDB datasets.

our segmentation effect is obviously better than that of TransUNet; from the second column, the extension of purple is better than that of TransUNet, and there is no vacancy in the blue part; from the third column, there is a semicircle in the yellow part, and the vacancy in red is smaller than that of TransUNet, etc. It is evident that DA-TransUNet outperforms TransUNet in segmentation quality. In summary, DA-TransUNet significantly surpasses TransUNet in segmenting the left kidney, right kidney, spleen, stomach, and pancreas. It also offers superior visualization performance in image segmentation.

We simultaneously took DA-TransUNet in five datasets, CVC-ClinicDB, Chest Xray Masks and Labels, ISIC2018-Task, kvasir-instrument, and kvasir-seg, and compared it with some classical models (see table 2). In the table, the values of IOU and Dice of DA-TransUNet are higher than TransUNet in all five datasets, CVC-ClinicDB, Chest Xray Masks and Labels, ISIC2018-Task, kvasir-instrument, and kvasir-seg. Also DA-TransUNet has the best dataset segmentation in four of the five datasets. As seen in the table, our DA-TransUNet has more excellent feature learning and image segmentation capabilities.

We also show the results of image segmentation visualization of DA-TransUNet in these five datasets, and we also show the results of the comparison models for the comparison. The visualization results for Chest X-ray Masks and Labels, Kvasir-Seg, Kvasir-Instrument, ISIC2018-Task, and CVC-ClinicDB datasets are presented in Figure7, Figure8, Figure9, Figure10, and Figure11, respectively. In the Figure, it can be seen that the segmentation effect of DA-TransUNet has a good performance. Firstly, DA-TransUNet has better segmentation results than TransUNet. In addition, compared with the four classical models of U-net, Unet++, Attn-Unet, and Res-Unet, DA-TransUNet has a certain improvement. It can be seen that the effectiveness of DA-TransUNet for model segmentation is not only confirmed in the Synapse dataset, but also in the five datasets (CVC-ClinicDB, Chest Xray Masks and Labels, ISIC2018-Task, kvasir-instrument, kvasir-seg). We further establish that DA-TransUNet excels in both 3D and 2D medical image segmentation.

Table 3: Results of the effect of the feature extraction module in the encoder and skip connections

	Encoder with DA	Skip with DA	DSC↑	HD↓
DA-TransUNet			77.48	31.69
DA-TransUNet		√	77.9	26.47
DA-TransUNet	√		79.13	34.32
DA-TransUNet	√	√	<b>79.80</b>	<b>23.48</b>

Table 4: Results of the effect of adding feature extraction blocks by skipping connections in different layers

	1st layer	2nd layer	3rd layer	DSC↑	HD↓
DA-TransUNet				77.48	31.69
DA-TransUNet		√		78.67	27.84
DA-TransUNet			√	78.44	31.91
DA-TransUNet				79.18	31.72
DA-TransUNet	√	√	√	<b>79.80</b>	<b>23.48</b>

#### 4.4 Ablation Study

We conducted ablation experiments on the DA-TransUNet model using the Synapse dataset to discuss the effects of different factors on model performance. Specifically, it includes: 1)DA-Block in Encoder. 2)DA-Block in Skip Connection.

##### 4.4.1 Effect of the DA-Block in Encoder And Skip Connection

In this study(see table3), we tested whether the inclusion of DA-Block at the coding layer and skip connections facilitates the model segmentation capability. Similarly, the distinction between DA-TransUNet (encoder with DA-Block) and DA-TransUNet (No DA-Block added) demonstrates a marked performance improvement. The incorporation of DA-Block in front of the Transformer in the encoder significantly elevates the system's effectiveness. This results in improved feature learning across all eight organs. By providing the decoder with more refined features can help the decoder to reduce feature disappearance during the upsampling process, reduce the risk of overfitting, and improve the stability of the model. Similarly, from DA-TransUNet(encoder with DA-Block) and DA-TransUNet(No DA-TransUNet added), it can be seen that the addition of DA-Block in front of Transformer in the encoder is also a significant improvement. Providing Transformer with more accurate features can greatly improve the ability of Transformer to learn features. Finally, based on the table3 it can be concluded that the addition of DA-Block before the skip connection and the Transformer layer in the encoder to extract features is effective. Adding DA-Blocks to skip connections refines the features for the decoder, while their inclusion in the encoder augments the Transformer's feature-learning abilities.

##### 4.4.2 Effect of adding DA-Blocks to skip connections in different layers

In this study(see table4), we tested at which layers of skip connections the addition of DA-Block achieves the greatest increase in model segmentation rate. As shown in the table DA-TransUNet (the first layer has DA blocks), DA-TransUNet (the second layer has DA blocks), DA-TransUNet (the third layer has DA block), DA-TransUNet(the first, second and third layers all have DA blocks), it can be seen that adding a DA-Block to any of the layers of the skip-connections has a significant improvement in the segmentation of the model, on top of adding a DA-block to the coding layer. Based on the table4, it can be seen that adding DA-Block in every layer of skip connection is the best effect. The traditional hopping connection only delivers the features from the encoding layer without considering the quality of the delivered features. According to the experiments, it can be concluded that delivering more accurate features to the decoding layer can improve the feature learning ability and image segmentation ability of the model to a greater extent.

### 5 Discussion

In this present study, we have discovered promising outcomes from the integration of dual-attention (DA) mechanism blocks with the Transformer and their combination with skip-connections. On the Synapse dataset, the Dice coefficient and Hausdorff distance (HD) reached 80.11% and 26.38mm, respectively. Furthermore, favorable outcomes were also achieved on five additional datasets.

First, the combination of Dual Attention Block (DA-Block) and Transformer can effectively improve the feature extraction ability and global information retention ability of Transformer. In the field of computer vision, ViT has successfully put Transformer to use and achieved impressive results. This proves the powerful feature extraction capability of the Transformer. In our experiments, combining dual-attention blocks with the Transformer demonstrates even better feature learning capabilities. Before the Transformer layer, we introduced DA blocks to provide more accurate features, which further enhanced the feature extraction capability of Transformer. Our experiments show that good results can be achieved by combining only the dual attention block with the Transformer (see Table3), which suggests that the dual attention block can further enhance the global feature extraction capability of the Transformer without creating redundancy.

Further, fusing DA-Block with skip connections can enhance the efficacy of skip connections to bridge over the semantic gap and help the decoder recover the feature map. In the traditional U-net[2] architecture, skip connections play a role in bridging the semantic gap between encoder and decoder. Initially, researchers successfully combined dual attention blocks and residual blocks into the first skip connection layer with promising results [5]. In our experiments, we introduced dual attention blocks only in the first skip-connection layer with good results (see Table4 ), thus confirming the effective feature extraction capability of skip-connections. However, we believe that adding dual attention blocks in only one layer is not sufficient to maximize the enhancement of the model. Further integration of dual-attention blocks into the second and third skip-connection layers resulted in notable performance gains at each layer. It is clear that

refinement of the features before feeding the preserved coded features into the decoding layer enhances information retention and improves image restoration by eliminating extraneous details.

Despite the advantages, our model has some limitations. Firstly, the introduction of the Dual Attention (DA) blocks contributes to an increase in computational complexity. This added cost could potentially be a hindrance in real-time or resource-constrained applications. Secondly, the decoder part of our model retains the original U-Net architecture. While this design choice preserves some of the advantages of U-Net, it also means that the decoder has not been specifically optimized for our application. This leaves room for further research and improvements, particularly in the decoder section of the architecture.

## 6 Conclusion

In this paper, we innovatively propose a DA-TransUNet model. To the best of our knowledge, this is the first study that combines DA blocks with Transformer for medical image segmentation tasks. By introducing DA blocks, the model provides more accurate features to the Transformer module in the coding layer, which improves the feature learning ability of the model and increases the segmentation capability of the model. We also incorporate the DA block into the skip connection layer, which reduces the semantic divide that exists in the traditional U-shaped encoder-decoder structure, thus improving the robustness of the model and reducing the risk of overfitting. Experimental results on six public datasets show that our proposed DA-TransUNet has good medical image segmentation capability. In addition, we believe that a large-scale replacement of CNNs in the U-shaped structure with Transformer modules, as in swin-unet, does not necessarily yield good results, and that a proper focus should be placed on the Transformer's own characteristics to improve the feature extraction capability.

## Acknowledgments

## References

- [1] Jonathan Long, Evan Shelhamer, and Trevor Darrell. Fully convolutional networks for semantic segmentation. In *Proceedings of the IEEE conference on computer vision and pattern recognition*, pages 3431–3440, 2015.
- [2] Olaf Ronneberger, Philipp Fischer, and Thomas Brox. U-net: Convolutional networks for biomedical image segmentation. In *Medical Image Computing and Computer-Assisted Intervention–MICCAI 2015: 18th International Conference, Munich, Germany, October 5–9, 2015, Proceedings, Part III 18*, pages 234–241. Springer, 2015.
- [3] Foivos I Diakogiannis, François Waldner, Peter Caccetta, and Chen Wu. Resunet-a: A deep learning framework for semantic segmentation of remotely sensed data. *ISPRS Journal of Photogrammetry and Remote Sensing*, 162:94–114, 2020.
- [4] Zongwei Zhou, Md Mahfuzur Rahman Siddiquee, Nima Tajbakhsh, and Jianming Liang. Unet++: A nested u-net architecture for medical image segmentation. In *Deep Learning in Medical Image Analysis and Multimodal Learning for Clinical Decision Support: 4th International Workshop, DLMIA 2018, and 8th International Workshop, ML-CDS 2018, Held in Conjunction with MICCAI 2018, Granada, Spain, September 20, 2018, Proceedings 4*, pages 3–11. Springer, 2018.
- [5] Zhao Shi, Chongchang Miao, U Joseph Schoepf, Rock H Savage, Danielle M Dargis, Chengwei Pan, Xue Chai, Xiu Li Li, Shuang Xia, Xin Zhang, et al. A clinically applicable deep-learning model for detecting intracranial aneurysm in computed tomography angiography images. *Nature communications*, 11(1):6090, 2020.
- [6] Ashish Vaswani, Noam Shazeer, Niki Parmar, Jakob Uszkoreit, Llion Jones, Aidan N Gomez, Łukasz Kaiser, and Illia Polosukhin. Attention is all you need. *Advances in neural information processing systems*, 30, 2017.
- [7] Alexey Dosovitskiy, Lucas Beyer, Alexander Kolesnikov, Dirk Weissenborn, Xiaohua Zhai, Thomas Unterthiner, Mostafa Dehghani, Matthias Minderer, Georg Heigold, Sylvain Gelly, et al. An image is worth 16x16 words: Transformers for image recognition at scale. *arXiv preprint arXiv:2010.11929*, 2020.
- [8] Jieneng Chen, Yongyi Lu, Qihang Yu, Xiangde Luo, Ehsan Adeli, Yan Wang, Le Lu, Alan L Yuille, and Yuyin Zhou. Transunet: Transformers make strong encoders for medical image segmentation. *arXiv preprint arXiv:2102.04306*, 2021.
- [9] Hu Cao, Yueyue Wang, Joy Chen, Dongsheng Jiang, Xiaopeng Zhang, Qi Tian, and Manning Wang. Swin-unet: Unet-like pure transformer for medical image segmentation. In *European conference on computer vision*, pages 205–218. Springer, 2022.

[10] Bennett Landman, Zhoubing Xu, Juan Eugenio Igelsias, M Styner, T Langerak, and A Klein. Segmentation outside the cranial vault challenge. In *MICCAI: Multi Atlas Labeling Beyond Cranial Vault-Workshop Challenge*, 2015.

[11] Jorge Bernal, F Javier Sánchez, Gloria Fernández-Esparrach, Debora Gil, Cristina Rodríguez, and Fernando Vilariño. Wm-dova maps for accurate polyp highlighting in colonoscopy: Validation vs. saliency maps from physicians. *Computerized medical imaging and graphics*, 43:99–111, 2015.

[12] Noel Codella, Veronica Rotemberg, Philipp Tschandl, M Emre Celebi, Stephen Dusza, David Gutman, Brian Helba, Aadi Kalloo, Konstantinos Liopyris, Michael Marchetti, et al. Skin lesion analysis toward melanoma detection 2018: A challenge hosted by the international skin imaging collaboration (isic). *arXiv preprint arXiv:1902.03368*, 2019.

[13] Philipp Tschandl, Cliff Rosendahl, and Harald Kittler. The ham10000 dataset, a large collection of multi-source dermatoscopic images of common pigmented skin lesions. *Scientific data*, 5(1):1–9, 2018.

[14] Debesh Jha, Pia H Smedsrød, Michael A Riegler, Pål Halvorsen, Thomas de Lange, Dag Johansen, and Håvard D Johansen. Kvasir-seg: A segmented polyp dataset. In *MultiMedia Modeling: 26th International Conference, MMM 2020, Daejeon, South Korea, January 5–8, 2020, Proceedings, Part II* 26, pages 451–462. Springer, 2020.

[15] Debesh Jha, Sharib Ali, Krister Emanuelson, Steven A Hicks, Vajira Thambawita, Enrique Garcia-Ceja, Michael A Riegler, Thomas de Lange, Peter T Schmidt, Håvard D Johansen, et al. Kvasir-instrument: Diagnostic and therapeutic tool segmentation dataset in gastrointestinal endoscopy. In *MultiMedia Modeling: 27th International Conference, MMM 2021, Prague, Czech Republic, June 22–24, 2021, Proceedings, Part II* 27, pages 218–229. Springer, 2021.

[16] Stefan Jaeger, Alexandros Karargyris, Sema Candemir, Les Folio, Jenifer Siegelman, Fiona Callaghan, Zhiyun Xue, Kannappan Palaniappan, Rahul K Singh, Sameer Antani, et al. Automatic tuberculosis screening using chest radiographs. *IEEE transactions on medical imaging*, 33(2):233–245, 2013.

[17] Sema Candemir, Stefan Jaeger, Kannappan Palaniappan, Jonathan P Musco, Rahul K Singh, Zhiyun Xue, Alexandros Karargyris, Sameer Antani, George Thoma, and Clement J McDonald. Lung segmentation in chest radiographs using anatomical atlases with nonrigid registration. *IEEE transactions on medical imaging*, 33(2):577–590, 2013.

[18] Ozan Oktay, Jo Schlemper, Loic Le Folgoc, Matthew Lee, Mattias Heinrich, Kazunari Misawa, Kensaku Mori, Steven McDonagh, Nils Y Hammerla, Bernhard Kainz, et al. Attention u-net: Learning where to look for the pancreas. *arXiv preprint arXiv:1804.03999*, 2018.

[19] Dhiraj Maji, Prarthana Sigedar, and Munendra Singh. Attention res-unet with guided decoder for semantic segmentation of brain tumors. *Biomedical Signal Processing and Control*, 71:103077, 2022.

[20] Changlu Guo, Márton Szemenyei, Yugen Yi, Wenle Wang, Buer Chen, and Changqi Fan. Sa-unet: Spatial attention u-net for retinal vessel segmentation. In *2020 25th international conference on pattern recognition (ICPR)*, pages 1236–1242. IEEE, 2021.

[21] Ali Jamali, Swalpa Kumar Roy, Jonathan Li, and Pedram Ghamisi. Transu-net++: Rethinking attention gated transu-net for deforestation mapping. *International Journal of Applied Earth Observation and Geoinformation*, 120:103332, 2023.

[22] Ze Liu, Yutong Lin, Yue Cao, Han Hu, Yixuan Wei, Zheng Zhang, Stephen Lin, and Baining Guo. Swin transformer: Hierarchical vision transformer using shifted windows. In *Proceedings of the IEEE/CVF international conference on computer vision*, pages 10012–10022, 2021.

[23] Ailiang Lin, Bingzhi Chen, Jiayu Xu, Zheng Zhang, Guangming Lu, and David Zhang. Ds-transunet: Dual swin transformer u-net for medical image segmentation. *IEEE Transactions on Instrumentation and Measurement*, 71:1–15, 2022.

[24] Yimin Yang and Siamak Mehrkanoon. Aa-transunet: Attention augmented transunet for nowcasting tasks. In *2022 International Joint Conference on Neural Networks (IJCNN)*, pages 01–08. IEEE, 2022.

[25] Yundong Zhang, Huiye Liu, and Qiang Hu. Transfuse: Fusing transformers and cnns for medical image segmentation. In *Medical Image Computing and Computer Assisted Intervention–MICCAI 2021: 24th International Conference, Strasbourg, France, September 27–October 1, 2021, Proceedings, Part I* 24, pages 14–24. Springer, 2021.

[26] Michal Drozdzal, Eugene Vorontsov, Gabriel Chartrand, Samuel Kadoury, and Chris Pal. The importance of skip connections in biomedical image segmentation. In *International Workshop on Deep Learning in Medical Image Analysis, International Workshop on Large-Scale Annotation of Biomedical Data and Expert Label Synthesis*, pages 179–187. Springer, 2016.

- [27] Kaiming He, Xiangyu Zhang, Shaoqing Ren, and Jian Sun. Deep residual learning for image recognition. In *Proceedings of the IEEE conference on computer vision and pattern recognition*, pages 770–778, 2016.
- [28] Gao Huang, Zhuang Liu, Laurens Van Der Maaten, and Kilian Q Weinberger. Densely connected convolutional networks. In *Proceedings of the IEEE conference on computer vision and pattern recognition*, pages 4700–4708, 2017.
- [29] Reza Azad, Ehsan Khodapanah Aghdam, Amelie Rauland, Yiwei Jia, Atlas Haddadi Avval, Afshin Bozorgpour, Sanaz Karimijafarbigloo, Joseph Paul Cohen, Ehsan Adeli, and Dorit Merhof. Medical image segmentation review: The success of u-net. *arXiv preprint arXiv:2211.14830*, 2022.
- [30] Huimin Huang, Lanfen Lin, Ruofeng Tong, Hongjie Hu, Qiaowei Zhang, Yutaro Iwamoto, Xianhua Han, Yen-Wei Chen, and Jian Wu. Unet 3+: A full-scale connected unet for medical image segmentation. In *ICASSP 2020-2020 IEEE international conference on acoustics, speech and signal processing (ICASSP)*, pages 1055–1059. IEEE, 2020.
- [31] Qiangguo Jin, Zhaopeng Meng, Changming Sun, Hui Cui, and Ran Su. Ra-unet: A hybrid deep attention-aware network to extract liver and tumor in ct scans. *Frontiers in Bioengineering and Biotechnology*, 8:605132, 2020.
- [32] Reza Azad, Maryam Asadi-Aghbolaghi, Mahmood Fathy, and Sergio Escalera. Bi-directional convlstm u-net with densley connected convolutions. In *Proceedings of the IEEE/CVF international conference on computer vision workshops*, pages 0–0, 2019.
- [33] Jun Fu, Jing Liu, Haijie Tian, Yong Li, Yongjun Bao, Zhiwei Fang, and Hanqing Lu. Dual attention network for scene segmentation. In *Proceedings of the IEEE/CVF conference on computer vision and pattern recognition*, pages 3146–3154, 2019.
- [34] Hyeonseob Nam, Jung-Woo Ha, and Jeonghee Kim. Dual attention networks for multimodal reasoning and matching. In *Proceedings of the IEEE conference on computer vision and pattern recognition*, pages 299–307, 2017.
- [35] Jianlou Si, Honggang Zhang, Chun-Guang Li, Jason Kuen, Xiangfei Kong, Alex C Kot, and Gang Wang. Dual attention matching network for context-aware feature sequence based person re-identification. In *Proceedings of the IEEE conference on computer vision and pattern recognition*, pages 5363–5372, 2018.
- [36] Zhao Shi, Chongchang Miao, U Joseph Schoepf, Rock H Savage, Danielle M Dargis, Chengwei Pan, Xue Chai, Xiu Li Li, Shuang Xia, Xin Zhang, et al. A clinically applicable deep-learning model for detecting intracranial aneurysm in computed tomography angiography images. *Nature communications*, 11(1):6090, 2020.
- [37] Yuming Cai, Haotian Li, Junyi Xin, and Guanqun Sun. Mlda-unet: Multi level dual attention unet for polyp segmentation. In *2022 16th ICME International Conference on Complex Medical Engineering (CME)*, pages 372–376. IEEE, 2022.
- [38] Haonan Wang, Peng Cao, Jiaqi Wang, and Osmar R Zaiane. Uctransnet: rethinking the skip connections in u-net from a channel-wise perspective with transformer. In *Proceedings of the AAAI conference on artificial intelligence*, pages 2441–2449, 2022.
- [39] Reza Azad, Mohammad T Al-Antary, Moein Heidari, and Dorit Merhof. Transnorm: Transformer provides a strong spatial normalization mechanism for a deep segmentation model. *IEEE Access*, 10:108205–108215, 2022.
- [40] Hongyi Wang, Shiao Xie, Lanfen Lin, Yutaro Iwamoto, Xian-Hua Han, Yen-Wei Chen, and Ruofeng Tong. Mixed transformer u-net for medical image segmentation. In *ICASSP 2022-2022 IEEE International Conference on Acoustics, Speech and Signal Processing (ICASSP)*, pages 2390–2394. IEEE, 2022.
- [41] Adam Paszke, Sam Gross, Francisco Massa, Adam Lerer, James Bradbury, Gregory Chanan, Trevor Killeen, Zeming Lin, Natalia Gimelshein, Luca Antiga, et al. Pytorch: An imperative style, high-performance deep learning library. *Advances in neural information processing systems*, 32, 2019.
- [42] Nabil Ibtehaz and M Sohel Rahman. Multiresunet: Rethinking the u-net architecture for multimodal biomedical image segmentation. *Neural networks*, 121:74–87, 2020.